

Toshiyuki Mori and John Drennan

Abstract

Present status and future prospect in the fuel cell field were introduced in this chapter. To explain the important future prospect in the materials science of fuel cells, the authors focused on the materials science in the solid oxide fuel cell field after briefly summarizing present status of research and development in the fuel cell field. Also the authors reintroduced the research results to highlight the important role of the ultimate analysis of microstructure, simulation for a reasonable conclusion of microanalysis, and the processing route design based on microanalysis. The usefulness of the combined approach of microanalysis, simulation, and the processing route design is presented.

1 Introduction

Fuel cells, as devices for direct conversion of the chemical energy of a fuel into electricity by the inverse reaction of the electrolysis of water, are one of the key enabling technologies for the transition to a sustainable society. This fuel cell device consists of electrolyte and electrodes (i.e., anode and cathode). The oxidation reaction of fuel takes place at the anode and creates the ion and electron.

T. Mori (✉)

Fuel cell materials group, Battery materials unit, National institute for materials science (NIMS), Tsukuba, Ibaraki, Japan

Hetro-interface design group, batteries and fuel cells field, global research centre for environment and energy based on nano-materials science, National institute for materials science (NIMS), Tsukuba, Ibaraki, Japan

e-mail: MORI.Toshiyuki@nims.go.jp

J. Drennan

Centre for Microscopy and Microanalysis, The University of Queensland, St. Lucia, QLD, Australia

e-mail: j.drennan@uq.edu.au

The electron moves around the external circuit and reaches the cathode to participate in the reduction reaction of oxygen or air. This electron in the external circuit can be used for generating electricity using the fuel cell devices. In this process, the mobile ion such as proton (H^+), hydroxyl ion (OH^-), carbonate ion (CO_3^{2-}), or oxide ion (O^{2-}) moves through the liquid or solid electrolytes to make water molecules at the anode side or cathode side.

The major types of fuel cells being developed are the proton exchange membrane fuel cells (PEMFCs), direct alcohol fuel cells (DAFCs), alkaline fuel cells (AFCs), phosphoric acid fuel cells (PAFCs), molten carbonate fuel cells (MCFCs), and solid oxide fuel cells (SOFCs).

PEMFCs are actively developed in the industry because of its low operating temperature ($<100^\circ C$), fast start-up/shutdown, and low local emissions. Automobile companies have tried to use this device as hybrid-type engines in their big vehicles such as shuttle bus and trailer. However, the development of PEMFCs slowed down due to unsatisfied durability, poor reliability, and its low power density (Miller and Bazylak 2011). It is still in the stage of demonstration applications. Alternatively, practical use for the residential-scale generator application of PEMFCs has already started in Japan. Gas Company started business for the development of the home energy management system in the family houses in Japan. It is one of the successful examples of practical use of PEMFCs. To make the best use of PEMFCs, the advanced PEMFCs for intermediate temperature operation (i.e., $100\text{--}200^\circ C$) have actively developed in the research field (Dupuis 2011).

For the development of the portable power generators, DAFCs (Yu et al. 2010) which are operated around $60^\circ C$ have been developed by the household electrical appliance manufacturers. In this case, fuel is alcohol (methanol (Scott et al. 1997) and ethanol (Neburchilov et al. 2007)) or ethylene glycol (Serov and Kwak 2010). Since DMFCs can use liquid fuels which are easy to store and transport for its operation, it is useful as a long-life battery in the portable electric devices. However, DMFCs have big problems such as the alcohol crossover from the anode side to the cathode side and its low power density as compared with PEMFCs. Also, the production cost of DMFCs is much higher than that of the conventional batteries in the portable electric devices. As a consequence, it appears to be hard to use DMFCs instead of the conventional batteries.

The AFCs (using aqueous KOH as electrolyte) were developed for the NASA Apollo space program. The AFCs systems were used for the shuttle missions in the space program. The main advantage of the AFCs is the high reaction kinetics at the electrodes in the alkaline condition. The non-precious metal electrodes such as Ni can be used for this device instead of Pt. Also, the operation temperature of the AFCs is relatively low (i.e., $23\text{--}70^\circ C$) compared with that of the PEMFCs and DMFCs. However, the mobility of OH will be drastically decreased by the reaction between electrolyte of the AFC and carbon dioxide (CO_2) in the air. To overcome this problem for the industrial applications such as the vehicle engine application, recent research has focused on the development of an AFC based on the anion-conducting polymer electrolytes to replace the KOH solution. Considerable efforts in this field improved the conductivity using hydroxyl ion in electrolyte and the

resistance against CO₂ of the system (Merle et al. 2011). However, conspicuous degradation of the performance of AFC has been observed due to the low chemical stability of the anion-conducting polymer electrolytes under the high pH condition.

PAFCs and MCFCs have a long development history for its practical use. However, it is hard to improve the efficiency of the generation of PEMFC (operation temperature: below 200°C) and poor durability of MCFCs (operation temperature: 650°C).

In the basic research field, micro-fuel cells using polymer electrolytes (Grinbergz and Skundin 2010) have attracted attention for the development of a new miniaturized power source which can withstand the development competition with the other batteries such as lithium-ion and lithium-polymer batteries. Also, other unique fuel cells named enzymatic fuel cells (or biofuel cells) which employ enzymes as catalysts have been examined for an implantable power source in the medical device application (Ivanov et al. 2010). Both fuel cells are only for the research purpose and are unlikely to use in the industry yet.

The efficiency of power generation of SOFCs is the highest of all the aforementioned fuel cell devices (Steele and Heinzel 2000). Also this device can create electricity using a variety of fuels. As a consequence of this, it is believed that SOFC is a promising fuel cell device for the development of sustainable society. However, this fuel cell has some technical problems such as unsatisfactory durability and reliability. To get the significant share of the electricity market, high durability (up to 100,000 h at the operation temperature) is required. To meet this challenge, the fuel cell material design is a key issue. Many fuel cell materials (i.e., solid electrolytes, cathodes, and anodes) have been developed in this field (Jacobson 2010; Sun et al. 2010). However, the old style SOFC material development did not create decisive solution for this challenge, so far. It is because the trial and errors for the development of SOFC materials lacks of the careful analysis of microstructure in the produced materials. For the development of the advanced SOFC materials, careful microanalysis and processing route design must be combined. Here, the authors reintroduce the previously reported results for the design of advanced SOFC materials based on micro-analysis (Mori et al. 2003, 2005, 2006, 2008; 2010; Ou et al. 2006, 2007; Ye et al. 2008, 2010; Wang et al. 2006; Li et al. 2010, 2011a, b, c, d, e, f).

2 Microanalysis of Bulk Structure in the Doped Ceria Solid Electrolytes and the Interface Structure Between Doped Ceria and Electrodes

Gd-doped ceria and Y-doped ceria electrolytes are representative electrolytes for the development of an intermediate temperature (300–500°C) operation of solid oxide fuel cell devices. In general, oxide ionic conductivity is described by

$$\sigma_i = (\sigma_i^0/T) \exp(-E_A/kT) \quad (60.1)$$

where T is absolute temperature, E_A is activation energy of oxide ion diffusion, k is Boltzmann constant, and σ_i^0 is intrinsic oxide ion conductivity.

Also E_A can be described by

$$E_A = \Delta H_m + \Delta H_a \quad (60.2)$$

where ΔH_m is migration enthalpy and ΔH_a is association enthalpy.

ΔH_m and ΔH_a correspond to the diffusion rate and stability of the oxygen vacancy clusters, respectively. It means that activation energy observed for Gd-doped ceria or Y-doped ceria using the Arrhenius plots has to be fixed value in each chemical composition. Alternatively, the observed E_A values have many variations in the previously reported papers. This clearly indicates that the detailed microstructural features of the prepared solid electrolytes should be taken into account for the design of the high-quality fuel cell materials.

To prepare the homogeneous and dense solid electrolytes, the soft chemical approaches such as coprecipitation method and sol-gel method have been used in many works. The well-dispersed and fine doped ceria solid solution powders have been prepared using the soft chemical approach. However, the dense doped ceria sintered bodies which were fabricated using the fine doped ceria powders included a heterogeneous microstructural feature. [Figure 60.1a](#) presents the scanning electron microscopy images observed for the fine Y-doped ceria powders and Y-doped ceria sintered bodies. Well-dispersed and fine Y-doped ceria powders which consist of the round shaped particles were synthesized using the ammonium carbonate hot coprecipitation method. Also the dense sintered bodies were fabricated by using those fine doped ceria powders. X-ray diffraction (XRD) profiles which were observed for the dense doped ceria sintered bodies consist of the simple fluorite-type phase. No other phases were observed in the XRD profiles ([Fig. 60.1a](#)).

Alternatively, the extra reflection and diffuse scattering were observed in the background of the selected area electron diffraction patterns recorded from the same sintered bodies ([Fig. 60.1b](#)). This indicates that small amount of different composition or different structure coexists in the fluorite phase of doped ceria. Since those heterogeneous structures are in the atomic scale, it would be hard to detect those nano-heterogeneous regions using the XRD analysis as shown in [Fig. 60.1a](#) (Mori et al. 2003; Ou et al. 2006, 2007). In the fuel cell research field, aforementioned nano-heterogeneous region is called as “micro-domain” or “nano-domain.” The average micro-domain size ranged from 5 to 10 nm. The heavy doped ceria system (i.e., more than 20% Y) includes a relatively large size micro-domain as compared with the light doped ceria system (i.e., less than 10% Y). The size and volume of the micro-domains in the samples strongly depend on the composition of the Y-doped ceria system, as shown in [Fig. 60.2](#).

The heterogeneous microstructure in 25% Y-doped ceria sintered body was characterized by using the analytical TEM as shown in [Fig. 60.3](#). The segregation of the Y dopants was observed in the nanoscale area. The micro-domain area observed in [Fig. 60.2](#) corresponded to the small heterogeneous area in [Fig. 60.3](#).

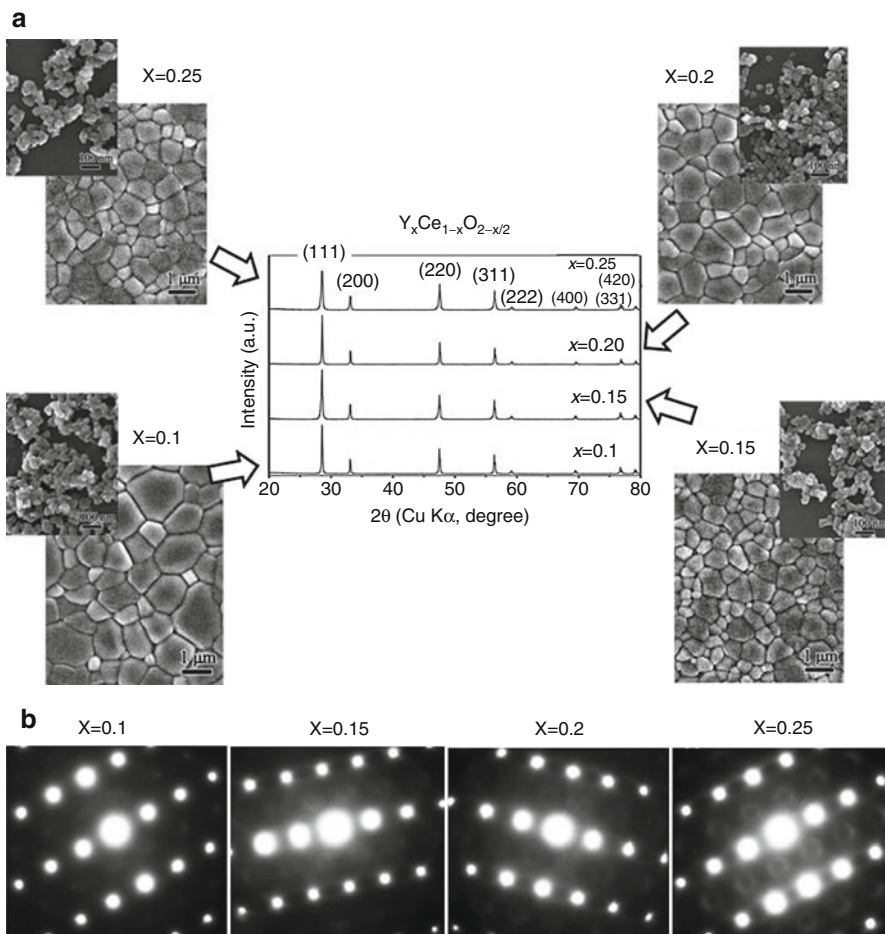


Fig. 60.1 (a) X-ray diffraction patterns and SEM images observed for Y-doped ceria. (b) Selected area electron diffraction patterns recorded from $Y_xCe_{1-x}O_{2-x/2}$ sintered bodies $\langle 112 \rangle_F$ zone

Since doped ceria has cubic symmetry, the shape of primary particles must be cubic. Also the secondary particles consist of a group of cubic-shaped primary particles. In the SEM images of Fig. 60.1, however, the surface of round-shaped particles of doped ceria was quite smooth. This suggests that the amorphous thin film covered the surface of secondary particles and nanoscale heterogeneity remains in the Y-doped ceria particles which were prepared by the coprecipitation method. During the sintering process of those easily sinterable powders, the nanoscale heterogeneity was developed and would make microdomain or nano-domain area in the sintered bodies. It was concluded that the micro-domain formation process strongly depends on the processing route, and the reliability of solid electrolytes

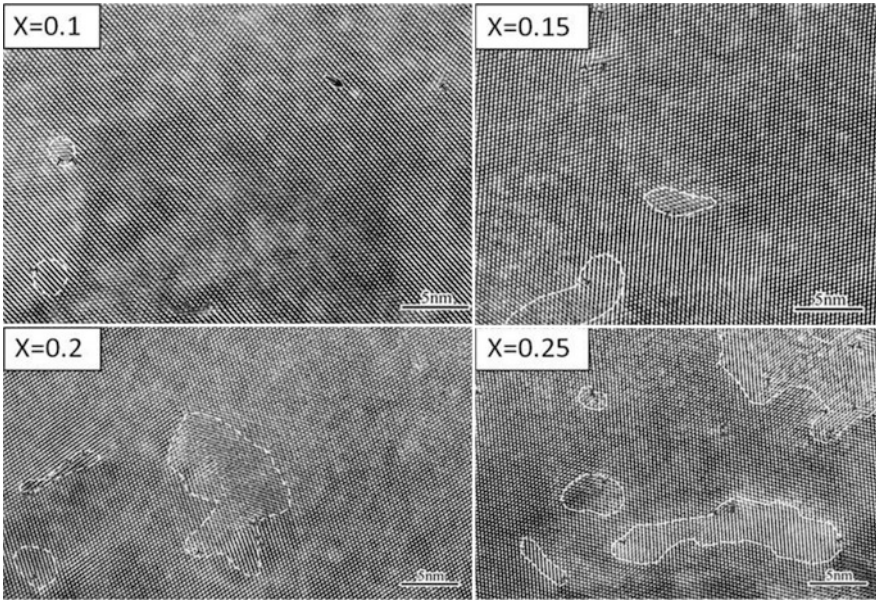


Fig. 60.2 High-resolution TEM images of $Y_xCe_{1-x}O_{2-x/2}$ sintered bodies. White dashed line areas indicate micro-domains

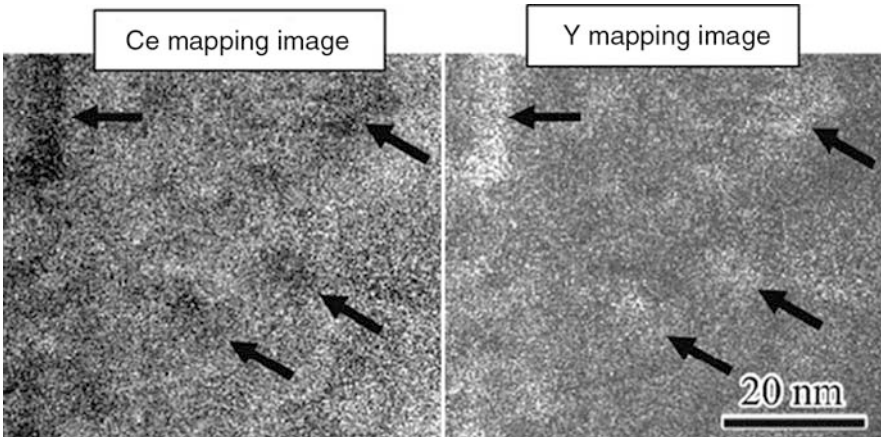


Fig. 60.3 EELS-TEM images observed for 25% Y-doped ceria sintered body which was sintered at 1,400°C. Black arrows indicate the agglomeration area of dopant at nanoscale

is affected by the volume fraction of micro-domain in the samples. Also similar microdomain structure can be observed in the Gd-doped ceria solid electrolyte series which are representative electrolyte material in SOFC (Mori et al. 2006, 2008, 2010; Ye et al. 2008). As a consequence of this, careful microanalysis and the processing

route design have to be combined for the development of high-quality solid electrolytes for the fuel cell application.

To design the oxide ion diffusion phenomenon in solid electrolyte, detailed defect structure analysis in the whole sintered body is required. The authors already characterized the microstructural features in detail using the EXAFS analysis technique (Wang et al. 2006) and the high power laser atom probe analysis technique (Li et al. 2010). Since both the EXAFS and laser atom probe analysis results agreed quite well with the TEM analysis results, the authors believe that electrolytes in the fuel cell devices must be designed using the combined approach of careful microanalysis and the processing route design.

Based on all microanalysis data, the authors tried to maximize the conducting property of the doped ceria solid electrolyte using the pulse electric current sintering (PECS) method (Mori et al. 2005). In the conventional sintering specimens, the big micro-domains with ordered structure of oxygen vacancies which sizes are more than 10 nm were dispersed into the whole specimen. Alternatively, micro-domain sizes became small into the PECS specimen. Also, electrolytic properties (i.e., conductivity and activation energy) were influenced by the change in microstructure, as

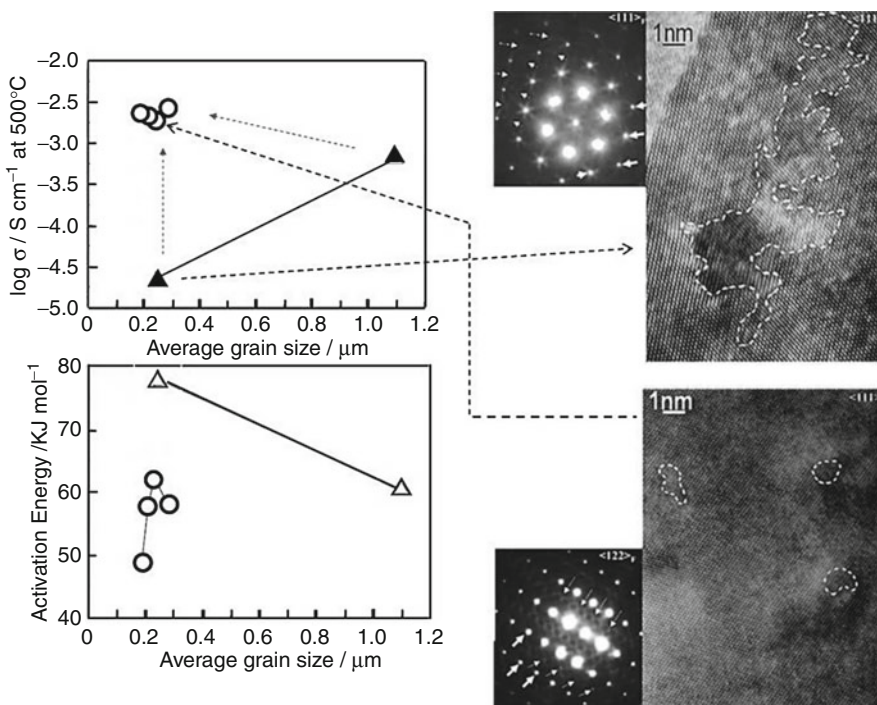


Fig. 60.4 Relationship between microstructure and electrolytic properties observed for PECS specimens and conventional sintering specimens, PECS specimen (Δ , \blacktriangle) and conventional sintering specimen (\circ); *bold white arrows* and *dashed white arrows* indicate the reflection from the fluorite structure and reflections from nano-domains into the fluorite phase, respectively

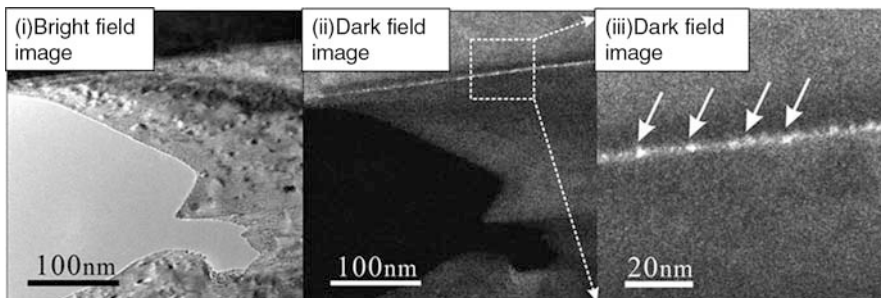


Fig. 60.5 Grain boundary analysis of Gd-doped ceria sintered body using high-resolution TEM

shown in Fig. 60.4. This clearly indicates that the combined method of microanalysis and the processing route design provide researchers and developers a big chance to see the breakthrough in the fuel cell field.

In the SOFC devices, the microstructure design in the grain boundary region and at the interface between electrolyte and electrodes (i.e., anode and cathode) is also quite important. The formation of nano-sized domains which sizes are less than approximately 2 nm in the grain boundary was observed using the high-resolution analytical TEM as shown in Fig. 60.5 (Li et al. 2011a). The continuous bright contrast of which width is within 2 nm was observed in the grain boundary. This bright continuous line means that the nano-sized domains with ordered structure of oxygen vacancies exist at the grain boundary. So far, this nano-heterogeneity was not always discussed well. As a consequence, reliability of solid electrolytes cannot be controlled well. To improve reliability of the fuel cell materials, this nanoscale heterogeneity should be recognized and fabricated with the high-quality solid electrolytes in the SOFC devices based on carefully microanalyzed data.

In addition, the interface design between solid electrolytes and electrodes (i.e., anode and cathode) is a key for the development of the SOFC devices.

Figure 60.6 presents the microanalysis results of the interface between Gd-doped ceria (GDC) solid electrolyte and Ni-GDC anode particles using STEM-EELS (Li et al. 2011b, d). The equal length diffusion between electrolytes and electrodes was observed. In general, interdiffusion into the hetero-interface can be observed. In the case of interdiffusion at the interface between electrolyte and electrode, Ni element which is the main component of the anode diffused into the electrolyte side through the grain boundary. The authors thought that the diffusion of the components of the electrolyte into the electrodes would be quite small. It can be a negligible level. However, almost same length diffusion from both sides were observed, even though atomic weight of each element (i.e., Ni:58.7, Gd:157.3, Ce:140.1) is quite different, and the diffusion constants of the Ni cation in the anode side and the Gd and Ce cations in the electrolyte side are different as well.

To conclude why the equal length diffusion which is named as “mutual diffusion” was observed at the interface, the detailed defect structure of the interface was characterized by using the high-resolution TEM. The TEM analysis suggests

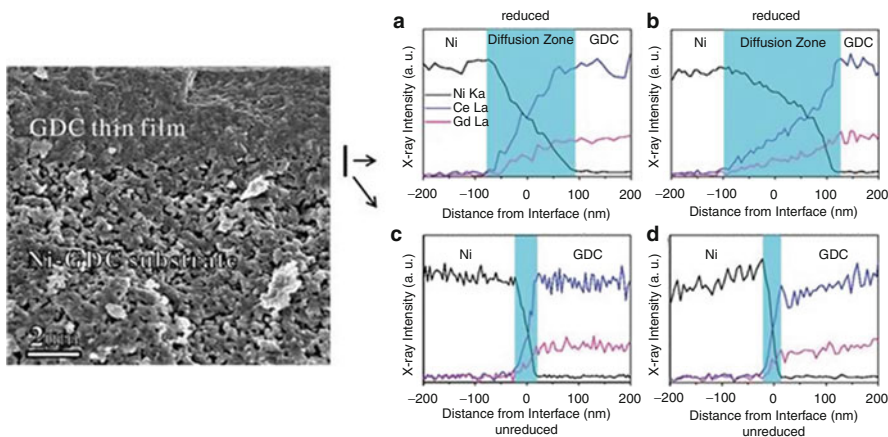


Fig. 60.6 Interface characterization of Gd-doped ceria using STEM-EELS analysis technique

that superstructure was formed in the interface area (Li et al. 2011b, c). Since superstructure consists of aggregation of the ordered oxygen vacancy clusters, the formation of the ordered oxygen vacancy clusters must be formed during the diffusion of components at the interface. In the case of the standard interdiffusion, there is no need to consider the superstructure formation. In the case of the diffusion phenomena at the interface of the fuel cell materials, the aforementioned equal length diffusion (i.e., “mutual diffusion”) proceeded with the superstructure formation. The rate-determining step would be the formation of superstructure at the interface. That is why the equal length diffusion was observed at the interface of electrolyte and anode in the SOFC device. Similar diffusion phenomena were observed around the interface between electrolyte and $\text{La}_{0.6}\text{Sr}_{0.4}\text{Co}_{0.8}\text{Fe}_{0.2}\text{O}_3$ cathode (Li et al. 2011a, b). Based on all the microanalysis results, the authors believe that microstructural features at the atomic scale for the design of high-quality SOFC devices should be taken into account.

3 Simulation of the Microanalysis Results

To develop a model for the design of high-quality fuel cell materials, computer simulation technique has to be applied for detail conclusion about the short-range ordering structure which is observed by TEM. Two representative examples of the simulation works from the author’s research team are reintroduced here (Ye et al. 2010; Li et al. 2011f). One is the simulation for the superstructure formation at the interface of electrolyte and anode (Ye et al. 2010). In general, the interaction of anion and cation in the ionic materials can be discussed using the Buckingham potential. The short-range ordering parameters of $\text{Ce}^{4+}-\text{O}^{2-}$, $\text{Ni}^{2+}-\text{O}^{2-}$, $\text{Gd}^{3+}-\text{O}^{2-}$, and $\text{O}^{2-}-\text{O}^{2-}$ were calculated using the Buckingham potential. Also the polarization parameters, space group, atomic coordinates, and lattice constants

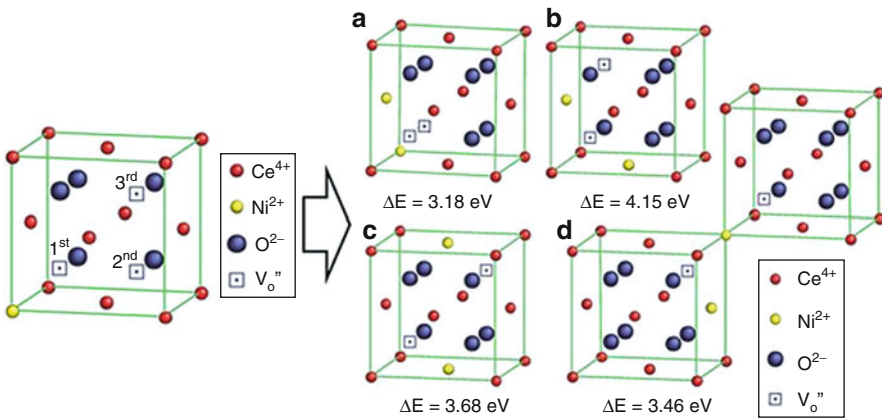


Fig. 60.7 Defect cluster energy calculation for a conclusion of super-structure formation in the interface

were used for the simulation. To discuss the stability of the ordered oxygen vacancy clusters, binding energy of clusters (ΔE) were estimated using

$$\Delta E = \Sigma E_{\text{isolated}} - E_{\text{cluster}} \quad (60.3)$$

where $\Sigma E_{\text{isolated}}$ is the formation energy of the isolated oxygen vacancy clusters and E_{cluster} is the formation energy of the ordered oxygen vacancy cluster. This equation indicates that stable cluster has high binding energy.

Various arrangements of the ordered oxygen vacancy clusters were examined (Ye et al. 2010). The clusters with the highest binding energy are shown in Fig. 60.7. It can be seen that the cluster shown in Fig. 60.7b is the most favorable one of all the clusters, indicating that adjacent oxygen vacancies in $(2\text{Ni}_{\text{Ce}}''2\text{V}_\text{o}'')$ are energetically favorable to be separated by $\langle 110 \rangle / 2$ (i.e., one-half of the distance between atoms in $\langle 110 \rangle$ direction into the unit cell).

This simulation result clearly indicates that the superstructure formation is the key step to conclude the mutual diffusion phenomenon for the interface design in the SOFC devices.

The second example is the simulation of the phase transformation from the conductive phase to the isolated phase in the solid electrolyte. In the case of Y_2O_3 stabilized ZrO_2 , Sc_2O_3 stabilized ZrO_2 , and Gd-doped ceria solid electrolytes, the isolated phase (i.e., tetragonal phase, monoclinic phase, or C-type rare earth phase) appeared in the conductive phase (i.e., the fluorite phase) of the aforementioned solid electrolytes which consist of the fluorite related structure during long-time operation at elevated temperature. For a long time, it was hard to understand why the phase transformation from the conductive phase to the isolated phase was observed in the electrolyte after long time operation test at the operation temperature. The author's research team tried to conclude this challenging subject using this simulation technique (Li et al. 2011f). The authors compared the binding

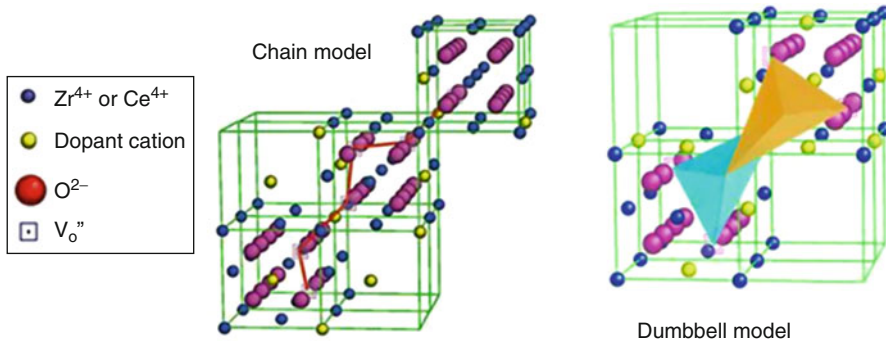


Fig. 60.8 Comparison of traditional cluster model (i.e., chain model) and dumbbell model

energies of the two cluster models (i.e., chain model and dumbbell model) in the fluorite structure as demonstrated in Fig. 60.8. In Gd-doped ceria, the dumbbell model which was proposed by the authors has the largest binding energy in the ceria matrix. Also, this simulation result indicates that low conductive phase can be observed when the dumbbell-type clusters are connected with each other and become a long stable chain in the material. This clearly indicates that combination of microanalysis, simulation, and the processing route design is the key approach to see a big breakthrough in the fuel cell materials science.

4 Summary

In this chapter, present status of the development of the fuel cell materials was explained at first. Then, the authors focused on solid oxide fuel cell materials because of its higher efficiency of the SOFC devices as compared with the other types of fuel cells. The authors reintroduced the previously reported results to introduce the advanced approach for the design of the breakthrough fuel cell materials in the SOFC field. In the research and development field of the SOFC technology, fuel cell materials were designed based on the ideal crystal structure model. However, heterogeneity at the atomic scale was observed in the bulk, grain boundaries, and interfaces in the SOFC devices. As briefly mentioned in this chapter, the authors believe that the combined approach of careful microanalysis, simulation, and the processing route design will provide researchers and developers a big chance to see a breakthrough in the SOFC field.

Acknowledgments

The authors are grateful to Professor Alastair N. Cormack (Alfred University, USA) for his kind advice in our simulation work. Also we appreciate the fruitful collaborative works to Professor Fei Ye (Dalian University of Technology, China),

Professor Ding Rong Ou (Chinese Academy of Sciences, China), Professor Jin Zou (The Queensland University, Australia), Dr. Graeme Auchterlonie (The Queensland University, Australia), and Dr. Zhipeng Li (National Institute for Materials Science, Japan).

5 Cross-References

- ▶ [Advanced Energy Devices-Lithium Ion Battery and High Energy Capacitor](#)
- ▶ [Advanced Japanese Service Design: From Elements to Relations](#)
- ▶ [Alternative Materials Development Utilizing Advanced Nanotechnology](#)
- ▶ [Computational Materials Science and Computer Aided Materials Design and Processing](#)
- ▶ [Design for Sustainability: the Interface of Sustainable Production and Consumption](#)

References

- A.C. Dupuis, Proton exchange membranes for fuel cells operated at medium temperatures: materials and experimental techniques. *Prog. Mater. Sci.* **56**, 289–327 (2011)
- V.A. Grinbergz, A.M. Skundin, Microfuel cells: modern state and future development (review). *Russ. J. Electrochem.* **46**(9), 963–978 (2010)
- I. Ivanov, T. Vidaković-Koch, K. Sundmacher, Recent advances in enzymatic fuel cells: experiments and modeling. *Energies* **3**, 803–846 (2010)
- A.J. Jacobson, Materials for solid oxide fuel cells. *Chem. Mater.* **22**, 660–674 (2010)
- F. Li, T. Ohkubo, Y.M. Chen, M. Kodzuka, F. Ye, D.R. Ou, T. Mori, K. Hono, Laser-assisted three-dimensional atom probe analysis of dopant distribution in Gd-doped CeO₂. *Scr. Mater.* **63**(3), 332–335 (2010)
- Z.P. Li, T. Mori, G. Auchterlonie, J. Zou, J. Drennan, Direct evidence of dopant segregation in Gd-doped ceria. *Appl. Phys. Lett.* **98**(9) (2011a). article number 093104
- Z.P. Li, T. Mori, G. Auchterlonie, Y. Guo, J. Zou, J. Drennan, M. Miyayama, Mutual diffusion and microstructure evolution at the electrolyte-anode interface in intermediate temperature solid oxide fuel cell. *J. Phys. Chem. C* **115**(14), 6877–6885 (2011b)
- Z.P. Li, T. Mori, G. Auchterlonie, J. Zou, J. Drennan, Superstructure formation and variation in Ni-GDC cermet anodes in SOFC. *Phys. Chem. Chem. Phys.* **13**(20), 9685–9690 (2011c)
- Z.P. Li, T. Mori, G. Auchterlonie, J. Zou, J. Drennan, Two types of diffusions at the cathode/electrolyte interface in IT-SOFCs. *J. Solid State Chem.* **184**(9), 2458–2461 (2011d)
- Z.P. Li, T. Mori, G. Auchterlonie, J. Zou, J. Drennan, Mutual diffusion occurring at the interface between La_{0.6}Sr_{0.4}Co_{0.8}Fe_{0.2}O₃ cathode and gd-doped ceria electrolyte during IT-SOFC cell preparation. *ACS Appl. Mater. Interfaces* **3**(7), 2772–2778 (2011e)
- Z.P. Li, T. Mori, F. Ye, D.R. Ou, J. Zou, J. Drennan, Structural phase transformation through defect cluster growth in Gd-doped ceria. *Phys. Rev. B* **84**, 1–5 (2011f). article number: 180201(R)
- G. Merle, M. Wessling, K. Nijmeijer, Anion exchange membranes for alkaline fuel cells: a review. *J. Membr. Sci.* **377**(1–2), 1–35 (2011)
- M. Miller, A. Bazylak, A review of polymer electrolyte membrane fuel cell stack testing. *J. Power Sources* **196**(2), 601–613 (2011)
- T. Mori, J. Drennan, Y. Wang, G. Auchterlonie, J.G. Li, A. Yago, Influence of nano-structural feature on electrolytic properties in Y₂O₃ doped CeO₂ system. *Sci. Technol. Adv. Mater.* **4**(3), 213–220 (2003)

- T. Mori, T. Kobayashi, Y. Wang, J. Drennan, T. Nishimura, J.G. Li, H. Kobayashi, Synthesis and characterization of nanohetero-structured Dy doped CeO₂ solid electrolytes using combination process of spark plasma sintering and conventional sintering. *J. Am. Ceram. Soc.* **88**(7), 1981–1984 (2005)
- T. Mori, J. Drennan, D.R. Ou, F. Ye, Design of high quality doped CeO₂ solid electrolytes with nano-hetero structure. *Int. J. Nucl. Res. (NUKLEONIKA)* **51**, S11–S18 (2006)
- T. Mori, R. Buchanan, D.R. Ou, F. Ye, T. Kobayashi, J.D. Kim, J. Zou, J. Drennan, Design of nano-structured ceria based solid electrolytes for development of IT-SOFC. *J. Solid State Electrochem.* **12**(7–8), 841–849 (2008)
- T. Mori, D.R. Ou, F. Ye, J. Zou, J. Drennan, A.N. Cormack, Nano-structure design of doped ceria solid electrolytes for intermediate temperature operation of solid oxide fuel cell. *Trans. Mater. Res. Soc. Jpn.* **35**(3), 431–441 (2010)
- V. Neburchilov, J. Martin, H. Wang, J. Zhang, A review of polymer electrolyte membranes for direct methanol fuel cells. *J. Power Sources* **169**(2), 221–238 (2007)
- D.R. Ou, T. Mori, F. Ye, M. Takahashi, J. Zou, J. Drennan, Microstructures and electrolytic properties of yttrium-doped ceria electrolytes: dopant concentration and grain size dependences. *Acta Mater.* **54**(14), 3737–3746 (2006)
- D.R. Ou, T. Mori, F. Ye, J. Zou, J. Drennan, Evidence of intragranular segregation of dopant cations in heavily yttrium-doped ceria. *Electrochem. Solid-State Lett.* **10**(1), 1–3 (2007)
- K. Scott, W. Taama, J. Cruickshank, Performance and modeling of a direct methanol solid polymer electrolyte fuel cell. *J. Power Sources* **65**(1–2), 159–171 (1997)
- A. Serov, C. Kwak, Recent achievements in direct ethylene glycol fuel cells. *Appl. Catal. B Environ.* **97**, 1–12 (2010)
- B.C.H. Steele, A. Heinzl, Materials for fuel-cell technologies. *Nature* **414**, 345–352 (2000)
- C. Sun, R. Hui, J. Roller, Cathode materials for solid oxide fuel cells: a review. *J. Solid State Electrochem.* **14**, 1125–1144 (2010)
- Y. Wang, H. Kageyama, T. Mori, H. Yoshikawa, J. Drennan, Local structures around Y and Ce cations in 10 mol% Y₂O₃ doped ceria ceramics by XAFS spectroscopy. *Solid State Ion.* **177**(19–25), 1681–1685 (2006)
- F. Ye, T. Mori, D.R. Ou, J. Zou, G. Auchterlonie, J. Drennan, Compositional and structural characteristics of nano-sized domains in gadolinium-doped ceria. *Solid State Ion.* **179**(21–26), 827–831 (2008)
- F. Ye, T. Mori, D.R. Ou, J. Zou, J. Drennan, S. Nakayama, M. Miyayama, Effect of nickel diffusion on the microstructure of Gd-doped ceria (GDC) electrolyte film supported by Ni-GDC cermet anode. *Solid State Ion.* **181**(13–14), 646–652 (2010)
- E.H. Yu, U. Krewer, K. Scott, Principles and materials aspects of direct alkaline alcohol fuel cells. *Energies* **3**, 1499–1528 (2010)